frontiers | Frontiers in Energy Research

TYPE Original Research
PUBLISHED 22 July 2022
DOI 10.3389/fenrg.2022.956443

Check for updates

OPEN ACCESS

EDITED BY
Krishna Kumar Yadav,
Madhyanchal Professional University, India

REVIEWED BY
Hu Pan,
Jiaxing University, China
Shiv Prasad,
Indian Agricultural Research Institute (ICAR), India

*CORRESPONDENCE
Yi-Hung Chen,
yhchen1@ntut.edu.tw

SPECIALTY SECTION
This article was submitted to Bioenergy and Biofuels, a section of the journal Frontiers in Energy Research

RECEIVED 30 May 2022
ACCEPTED 27 June 2022
PUBLISHED 22 July 2022

CITATION
Yuan M-H, Chen Y-H, Peng S-C, Chen L-Y, Chang C-Y, Santikunaporn M, Assavatesanuphap C and Lee Y-F (2022), Depression effect of the cold filter plugging point by blending of palm oil, palm stearin, and palm olein biodiesels in petrodiesels. *Front. Energy Res.* 10:956443. doi: 10.3389/fenrg.2022.956443

COPYRIGHT
© 2022 Yuan, Chen, Peng, Chen, Chang, Santikunaporn, Assavatesanuphap and Lee. This is an open-access article distributed under the terms of the Creative Commons Attribution License (CC BY). The use, distribution or reproduction in other forums is permitted, provided the original author(s) and the copyright owner(s) are credited and that the original publication in this journal is cited, in accordance with accepted academic practice. No use, distribution or reproduction is permitted which does not comply with these terms.

Depression effect of the cold filter plugging point by blending of palm oil, palm stearin, and palm olein biodiesels in petrodiesels

Min-Hao Yuan[1], Yi-Hung Chen[2]*, Siou-Chih Peng[2], Lu-Yen Chen[3], Ching-Yuan Chang[4], Malee Santikunaporn[5], Channarong Assavatesanuphap[6] and Yi-Fa Lee[7]

[1]Department of Occupational Safety and Health, China Medical University, Taichung, Taiwan, [2]Department of Chemical Engineering and Biotechnology, National Taipei University of Technology, Taipei, Taiwan, [3]Department of Energy Engineering, National United University, Miaoli, Taiwan, [4]Graduate Institute of Environmental Engineering, National Taiwan University, Taipei, Taiwan, [5]Department of Chemical Engineering, Thammasat School of Engineering, Thammasat University, Pathum Thani, Thailand, [6]Department of Mechanical Engineering, Thammasat School of Engineering, Thammasat University, Pathum Thani, Thailand, [7]Chant Oil Co., Ltd., New Taipei City, Taiwan

The cold filter plugging point (CFPP) has been widely used to evaluate the low-temperature operability of neat biodiesel and biodiesel–petrodiesel blends in many European and Asian countries. In this study, six kinds of palm biodiesels (palm oil, palm stearin, and palm olein methyl esters in undistilled and distilled forms) in two Taiwanese major petrodiesels (CPC and FPCC) were adopted to examine their CFPP from 100 vol% biodiesel (B100) to 100 vol% diesel (D100 or B0). The results showed that the CFPPs of B2–B12 for CPC and B10–B12 for FPCC were consistently lower than the initial CFPP of D100 from all the palm biodiesel. The most significant depression effect of CFPP was found in B10, where the CFPP of B10 was substantially reduced to about 3–7°C as compared with those of D100 in both petrodiesels. The CFPP of B10 was from –7 to –8°C in CPC and –10 to –13°C in FPCC, where CFPPs of CPC and FPCC neat fuels were –4 and –6°C, respectively. Undistilled palm oil and palm olein biodiesels exhibited stronger depression effect than distilled palm biodiesels at the same level of biodiesel–petrodiesel blends and covered a wider range for the depression effect. Even though the CFPP of palm biodiesels falls outside the limit of Taiwanese B100, the finding revealed that a low blending of B2–B12 of palm biodiesels can result in a better and satisfactory CFPP of biodiesel–petrodiesel admixture that meets the diesel standard CNS 1471.

KEYWORDS

palm biodiesel, cold filter plugging point, low-temperature operability, biodiesel–petrodiesel blend, depression effect

1 Introduction

Bioenergy is the largest renewable energy source globally that can be used in all sectors and plays an important role to reach the net zero emission by 2050 (Kung et al., 2022). Among them, biodiesel is regarded as a major alternative fuel and has been widely used as a blend component in petrodiesel by more than 60 countries (Lane, 2015). About 48 billion liters of biodiesel were consumed in 2020, where the top three biodiesel-consuming countries were the European Union (EU), United States, and Indonesia (OECD/FAO, 2021). Biodiesel consists of a mixture of fatty acid methyl esters (FAME) obtained from the transesterification of triglycerides or the esterification of free fatty acids by various oil-containing crops, waste cooking oil, grease, or other types of feedstocks. It enables significantly reduced emission of air pollutants such as hydrocarbons, carbon monoxide, and particulate matter, albeit alongside a slight increase in nitrogen oxide emissions (Agarwal, 2007; Luque et al., 2010; Hoekman et al., 2012; Jambulingam et al., 2019). Moreover, the carbon dioxide released into the atmosphere by biodiesel combustion is offset by the carbon dioxide absorbed from growing plants or feedstocks used to produce the fuel. Biodiesel can be used in the neat form by modern diesel engines without requiring significant modifications (Agarwal, 2007; Hoekman et al., 2012). Nevertheless, it is more commonly used as a blend component in petrodiesel at mandated levels of 2 vol% (B2) to 20 vol% (B20) (Lane, 2015). In Taiwan, renewable energy policy for B2 biodiesel fuel had been launched from 2010–2014 while the annual biodiesel production was 9.6 ML in 2013. Since mid-2014, the mandated biodiesel policy was terminated due to operational and maintenance concerns from corporate users (Chung, 2018).

Among the biodiesel feedstock, oil palm is the fastest-growing and least expensive, and its production can be economically viable even without direct subsidies (Demirbas, 2009; Elbehri et al., 2013). In addition, a booming palm oil business in Malaysia and Indonesia provides a promising route out of poverty for small-scale farmers, as smallholders represent a significant portion of the current expansion (Gilbert, 2012; Kongsager and Reenberg, 2012). Hence, future expansion of biodiesel-use mandates largely has to meet an expanded demand for oil palm, if second, third, and advanced generation biofuels are still struggled to be commercially viable (Lee and Lavoie, 2013; Najjara and Abu-Shamleh, 2020; Lin and Lu, 2021).

Palm biodiesels have met most of the strict quality specifications that ensure smooth performance, except cold flow properties, which are inferior for low-temperature operability (Benjumea et al., 2008; Hazrat et al., 2020; Knothe, 2008; Knothe, 2009). The cold flow properties of biodiesel and all diesel fuels are evaluated using the cloud point (CP), cold filter plugging point (CFPP), pour point (PP), and the low temperature flow test (LTFT) (Hazrat et al., 2020; Knothe, 2008). Among them, CFPP, an estimate of the lowest temperature at which a fuel gives smooth flow in certain fuel systems, is widely used in biodiesel specifications in most European and Asian countries. The LTFT, which is used to predict the operability of engine fuel-systems under severe low-temperature conditions, is used mainly in North America. Numerous studies have shown that the poor cold flow properties of palm biodiesel are caused mainly by the high content of long-chain saturated FAMEs, given that CFPP of palm methyl ester is about 10–15°C (Knothe, 2008; Knothe, 2009). For the CFPP specification for B100, EU countries is set from 5 to −20°C depending on the time of the year and the location, and Taiwan requires the CFPP of 0 °C around all year and anywhere. Blending of biodiesels with a high level of unsaturation and better cold flow properties (e.g., rapeseed, soybean, and Jatropha methyl esters) has shown promising results in improving the CFPP of highly saturated palm biodiesel (Echim et al., 2012; Moser, 2008; Sarin et al., 2010; Yuan et al., 2017). Other improvement techniques include blending with a fuel (e.g., kerosene or ethanol), utilization of additives (PP depressants or cold-flow improvers), winterization, and other treatments (Dunn et al., 1996; Gonzalez-Gomez et al., 2002; Liu, 2015). Liu (2015) summarized that blending with kerosene or ethanol would reduce the freezing point of biodiesel by a large extent. Furthermore, treatment with chemical additives usually was applied at low concentrations. Winterization effectively removes the high-freezing point components by partial crystallization (Gonzalez-Gomez et al., 2002). Although these additional approaches can modify palm biodiesels to reach satisfactory cold flow properties, they may also undermine the environmental benefits in terms of the energy ratio and CO_2 emission, as well as reduce the commercial viability of palm biodiesels.

Apart from the abovementioned methods, blending biodiesel with conventional diesel fuels at the mandated low blend level may not adversely affect the cold flow properties of petrodiesel (Benjumea et al., 2008; Dunn et al., 1996; Dunn and Bagby, 1995; Moser, 2008). In fact, the cold flow properties (CP, CFPP, and PP) at a low-blend level (B1–B5) are equivalent regardless of whether the biodiesel sample contains a high percentage of long-chain saturated FAME (Moser, 2008). Moreover, a few studies have noted that conventional diesel blending with some feedstock biodiesel at certain low levels would lower CFPPs in compassion of neat diesel fuel. Richards et al. (2007) showed that blending of 1% beef tallow and lard methyl esters (both with a CFPP of 12°C) with Slovnaft diesel (CFPP of −6°C) resulted in CFPPs of −10 and −9°C, respectively, which are lower than those of the pure constituents. Similar observations have been made with blends of low-CFPP fuels of rapeseed methyl ester (−18°C) and diesel (−34°C) at B5–B20 (Kleinová et al., 2007) and with blends of rapeseed (−8°C) or soybean–palm admixture (0°C) methyl esters with Bulgarian diesel (−10°C) at B10–B20 (Sharafutdinov et al., 2012). The former (Kleinová et al., 2007)

and latter (Sharafutdinov et al., 2012) blends have CFPPs below −40°C and below −15°C, respectively. Lowering of the CFPP has also been observed with a blend of 20% palm methyl ester and Chinese −10PD fuel (Chen et al., 2013). This phenomenon may be explained by the depression or inhibition of crystal growth and agglomeration; some compounds from biodiesel and conventional diesel may hinder the agglomeration of crystals and therefore retard crystal growth with decreasing ambient temperature (Sharafutdinov et al., 2012). However, the depression effect of CFPP by blending different types of palm biodiesels with Asian country's diesel fuels is rarely discussed.

To fill up this gap, this study examines the CFPP of palm methyl ester blends with two major Taiwanese diesel fuels by using six kinds of palm biodiesel samples, including palm methyl ester (PME), palm stearin methyl ester (PSME), and palm olein methyl ester (POME) in undistilled and distilled forms. The effects of CFPP on FAMEs for neat palm biodiesels and the CFPP depression of petrodiesel due to the blending of palm biodiesels were presented and elucidated. On the basis of current findings, implications for future research and regulatory practice on the CFPP of palm biodiesel–petrodiesel blends were discussed.

2 Materials and methods

2.1 Materials

Three feedstocks were used in biodiesel production. Palm oil, palm stearin, and palm olein were supplied by Ting Hsin Int. Group (Taipei, Taiwan). Methanol (methyl alcohol, 99.7% purity) was obtained from Shiny Chemical Industrial Co. (Kaohsiung, Taiwan). Sodium methoxide (30% purity) was provided by Evonik Industries (North Rhine-Westphalia, Germany). Ultra-low-sulfur super petrodiesels (ULSDs) were purchased directly from gas stations of the Chinese Petroleum Corporation (CPC) and Formosa Petrochemical Corporation (FPCC) in Taipei. The fuel properties of Taiwanese diesel had to satisfy the specifications of CNS 1471 (similar to EN 590), that is, the CFPP for petrodiesel and B2 fuels must be lower than −3°C.

2.2 Biodiesel preparation

Biodiesel is synthesized mainly through the transesterification process. We performed methanolysis of triacylglycerols from different feedstocks under optimal reaction conditions in a stirred batch reactor: a methanol/feedstock molar ratio of 6:1, a rotational speed of 1,000 rpm, a reaction temperature of 65–70°C, a catalyst (CH_3ONa) dosage of 0.4 wt% based on the oil weight, and a reaction time of 2 h. The preparation procedures were similar to previous studies (Chen et al., 2010; Pan et al., 2020; Pan et al., 2022).

The samples were left to settle overnight to allow phase separation. Subsequently, the crude methyl esters were washed with deionized water to remove any residual methanol or glycerol and then subjected to vacuum dewatering to obtain purified and dried FAME. For the distillation process, 500 ml of each type of biodiesel was distilled under reduced pressure (3–4 Torr) at about 180–225°C and then stored at room temperature.

2.3 Preparation of biodiesel blends with petrodiesel

Precisely measured amounts of PME, PSME, POME, and their distilled samples (namely, PME-D, PSME-D, and POME-D) were blended with the ULSD fuels with continuous stirring to ensure homogeneity.

CPC diesel mixtures were blended according to volumes corresponding to B2, B6, B8, B10, B12, B15, B20, B30, B40, B50, B60, B70, B80, and B90, where BX represents a blend of X% biodiesel and (100–X)% ULSD by volume. To verify the trend of the CFPP, the FPCC, the second gasoline and diesel fuel provider in Taiwan, diesel fuel was used to prepare B2, B6, B8, B10, B20, and B50 of palm biodiesel–petrodiesel blends.

2.4 Analytical methods

The contents of FAME and free glycerol and mono-, di-, and tri-glycerides in the neat biodiesels were determined using gas chromatography according to EN 14103 and EN 14105, respectively (Chen et al., 2010). The composition and quantity of FAME, glycerol, and glycerides were analyzed using an Agilent 6890N and Agilent 7890 gas chromatograph (Santa Clara, CA, United States) with a flame ionization detector. A VB-WAX capillary column (Western Analytical Products, Inc., Murrieta, CA, United States) with a length of 30 m, a film thickness of 0.25 mm, and an internal diameter of 0.32 mm was used. Nitrogen was used as carrier gas and as auxiliary gas for a flame ionization detector. The injection volume of the sample was 1.0 μL. The FAME profile of the blend samples was calculated by using the densities of neat biodiesel and diesel fuels, which were measured with a density meter (DMA 35, Anton Paar, Graz, Austria).

Biodiesel properties of acid value and iodine value were determined using an automatic potentiometric titrator (KEN AT-510, Japan) according to EN 14104 and EN 14111, respectively (Pan et al., 2020; Pan et al., 2022). The acid value uses a dilute ethanolic KOH solution with phenolphthalein as indicator. The iodine number uses Wijs reagent to determine the number of double bonds of the fatty acids.

The CFPP of the samples was determined according to EN 116 and ASTM D6371 by using a circulating bath (Firstek B10/-40; Seton Finite Co., Kaohsiung, Taiwan) and test jars (Koehler,

TABLE 1 Compositions, colors, and other properties of distilled and non-distilled palm biodiesels.

Fatty acid methyl esters (FAMEs, wt%)	PME	PME-D	PSME	PSME-D	POME	POME-D
C14:0	1.2	1.2	1.6	1.5	1.2	1.4
C16:0	46.6	46.3	64.6	63.9	40.5	44.1
C16:1	0.2	0.2	0.1	0.2	0.2	0.2
C18:0	4.5	4.4	4.7	4.8	4.4	3.9
C18:1	37.6	37.4	23.2	23.9	42	39.5
C18:2	9.4	10	5.3	5.4	10.8	10.1
C18:3	0.2	0.2	0.2	0.1	0.6	0.4
C20:0	0.4	0.4	0.3	0.3	0.4	0.3
Free glycerol (FG) and glycerides (Glyc) (wt%)						
FG	0.01	0.01	0.005	0.022	0.007	0.11
Mono-glyc: 0.8[a] and 0.7[b] max	0.51	0.107	0.358	0.07	0.382	0.177
Di-glyc	0.077	–	0.093	–	0.113	–
Tri-glyc	–	–	–	–	0.048	–
Total glyc: 0.25 max.[a,b]	0.154	0.037	0.112	0.04	0.128	0.057
Properties of biodiesel						
CFPP (°C): 0 max.[a]	17	18	18	18	12	13
Ester content (%): 96.5 min.[a,b]	99.0	99.9	98.6	99.8	99.0	99.5
Acid value (mg KOH/g): 0.5 max.[a,b]	0.10	0.11	0.10	0.14	0.13	0.16
Iodine value (g I_2/100 g): 120 max.[a,b]	48.5	48.7	30.4	30.4	54.8	53.3
Oil colors-Gardner (–)	0.5	0.0	0.9	0.1	0.6	0.1
Oil colors-iodine (–)	0.7	0.0	1.0	0.1	0.8	0.2

Note: Property specification of neat biodiesel from EU EN 14214[a] and Taiwan CNS, 15072[b]; max. and mix. represent the upper and lower bounds of values to be met, respectively.

Holtsville, NY, United States). The observed CFPP was deemed as the lowest temperature at which a 45 ml sample safely passed through the filter within 60 s at an interval of 1°C. The duplicate experiments were performed, and the repeatability of the CFPP measurement for the samples was ±1°C. To compare the appearance of distilled and distilled biodiesel, oil color was measured according to ASTM D1500 using a LICO 620 Colorimeter (Hach Lange Ltd., Manchester, United Kingdom) with Gardner and iodine color scales.

3 Results and discussion

3.1 Compositions, cold filter plugging point, and other properties of neat palm biodiesels

The FAME compositions and some biodiesel properties of the six neat samples are summarized in Table 1. The main differences among the palm oil, palm stearin, and palm olein biodiesels were observed in the amounts of palmitic acid (C16:0) and oleic acid (C18:1). It is noted that palm stearin is the more solid fraction of palm oil after fractionation at a controlled temperature and the residual liquid fraction is palm olein (Lim, 2012). Therefore, the highest content of C16:0 was observed in PSME (63.9–64.6%), as expected. The C16:0 contents of PME and POME were 46.3–46.6% and 40.5–44.1%, respectively. Higher C16:0 contents come with lower C18:1. POME had the lowest C16:0 content and the highest C18:1 content (39.5–42.0%).

For CFPP of biodiesel, the result indicated that the CFPPs of PME and PSME in undistilled and distilled forms were about 17–18°C. Since the saturated FAMEs have higher melting points (MP) than those of unsaturated FAMEs with the same chain length, the higher contents of saturated FAMEs usually result in higher value of CFPP. Therefore, POME with the lowest C16:0 and the highest C18:1 content exhibits the lowest CFPP (12°C).

As shown in Table 1, the obtained mono glycerol, total glycerides, ester content, acid, and iodine values all satisfied the biodiesel specification of neat biodiesel from European EN 14214 and Taiwan CNS 15072. After the distillation process, the oil color and mono-, di-, and tri-glycerides contents of the samples substantially decreased. Then, the ester content slightly increased about 0.5–1.2%. The FAME composition and the other properties remain similar between distilled and undistilled palm biodiesels, although all distilled samples become

TABLE 2 CFPP prediction of unblended palm biodiesels in distilled and non-distilled forms.

No	Reference	Mathematical models	Calculated CFPP (°C)						AAD $n = 6$	RMSD $n = 6$	AAD $n = 4$	RMSD $n = 4$
			PME	PME-D	PSME	PSME-D	POME	POME-D				
Best fitting models validated by Dunn [31]												
1	Echim M2 [20]	CFPP = 0.5024 (ΣSFAME) − 12.569	13.9	13.7	23.2	22.9	10.8	12.4	3.77	5.20	1.26	1.38
2	Jeong M1 [32]	CFPP = 0.449 (ΣSFAME) − 9.918	13.7	13.6	22.1	21.7	11.0	12.4	2.85	3.22	2.33	2.82
3	Moser M2 [18]	CFPP = 0.51 (ΣSFAME) − 11.3	15.6	15.4	25.0	24.7	12.4	14.0	3.20	4.16	1.38	1.60
4	Chen [33]	CFPP = 61.2 ($yc_{16:0}$) + 0.81 ($yc_{18:3}$) − 11.7	16.8	16.6	27.8	27.4	13.1	15.3	4.03	5.68	1.23	1.44
5	Serrano M1 [34]	CFPP = −0.12 ($\Sigma C_{4:0}$-$C_{14:0}$) + 0.47 ($\Sigma C_{16:0}$-$C_{24:0}$) − 0.14 (ΣUFAME)	17.4	17.2	28.5	28.1	13.6	15.5	4.33	6.08	1.35	1.57
6	Serrano M2 [34]	CFPP = −26 + 5.76 ($\Sigma C_{16:0}$-$C_{24:0}$)$^{0.5}$	15.3	15.2	22.1	21.8	12.8	14.0	2.36	2.70	1.57	1.76
7	Yuan M1 [21]	CFPP = −13.837 + 0.149($Y_{C14:0}$) + 0.537($Y_{C16:0}$) + 0.741($Y_{C18:0}$) + 3.037($Y_{C20:0}$)	15.9	15.7	25.5	25.2	12.6	13.9	3.25	4.38	1.21	1.38
8	Yuan M2 [21]	CFPP = −13.784+1.269($YC_{C14:0}$) + 0.498($Y_{C16:0}$) + 0.621($Y_{C18:0}$) + 3.281($Y_{C20:0}$)	15.1	14.8	24.3	23.9	12.0	13.4	2.96	3.85	1.38	1.86
9	Yuan M3 [21]	CFPP = −13.688+0.518($Y_{C16:0}$) + 0.778($Y_{C18:0}$) + 3.066($Y_{C20:0}$)	15.2	14.9	24.4	24.1	11.9	13.1	2.91	3.87	1.26	1.78
10	Sarin M2 [19]	CFPP = −0.561 (ΣUFAME) + 43.967	17.4	17.2	27.8	27.4	14.0	15.9	4.21	5.74	1.51	1.79
Other models												
11	Moser M3 [18]	CFPP = −0.221(IV) + 22.031	11.3	11.3	15.3	15.3	9.9	10.3	3.77	4.16	4.31	4.73
12	Dunn M2 [31]	CFPP = $\{(-1.31 \times 10^{-4})\ln(y_{16:0}) + 3.42 \times 10^{-3}\}^{-1}$−273.15	10.9	10.9	14.4	14.3	9.5	10.4	4.27	4.61	4.59	5.02

Note: AAD is the average absolute deviation (average of |CFPPcal—CFPPexpl) by an individual model. RMSD is the root-mean-square deviation. SFAME and UFAME represent the saturated and unsaturated FAME, respectively content. Cm: n represents fatty acid with the carbon number "m" and unsaturated bond.

10.3389/fenrg.2022.956443

transparent and colorless (ASTM D1500 color scale <0.5). Note that the commercial biodiesel is often used in distilled form for obtaining a colorless transparent product.

3.2 Cold filter plugging point calculation of unblended palm biodiesels with high C16:0

Correlations of CFPP have been extensively developed for neat biodiesels and their admixture derived from major feedstocks (e.g., palm, canola, soybean, rapeseed, and Jatropha oils). To the best of our knowledge, palm stearin was seldom used for the establishment of CFPP models. PSME possesses quite high content of C16:0 (63.9–64.6%), which is possibly out of range of their selected predictive variables; therefore, it would be interesting to validate the robustness and applicability of current available CFPP models for PSME.

Dunn (2020) has reviewed the performance of 26 CFPP models of biodiesel and classified their selected predictor variables into four categories: 1) total of saturated and unsaturated FAME content, 2) one or a combination of individual FAME, 3) long-chain saturation factors with weight coefficients of melting point or specific number, and 4) degree of unsaturation, iodine value, average FAME chain length, etc. Then, ten best performance models proposed by Echim et al. (2012), Jeong et al. (2008), Moser (2008), Chen et al. (2010), Serrano et al. (2014), Yuan et al. (2017), and Sarin et al. (2010) were nominated based on the average absolute deviation (AAD) and root-mean-square deviation (RMSD) ≤ 2 from their experimental and calculation data pairs. Note that their predictor variables were all within the categories 1 and 2. In this analysis, the ten well-received models and validation procedures from Dunn (2020) were adopted to calculate the CFPP of PME, PSME, and POME. The descriptions of the selected mathematical models and their prediction results are summarized in Table 2.

The calculation results showed that all ten models overestimated the CFPP of PSME from 21.8 to 28.5°C, and their AAD and RMSD numbers were above 2 with the PSME (n = 6). The best estimate is by Serrano M2 with AAD and RMSD ≤3, where it is a non-linear 0.5 order equation by the sum of long-chain saturated FAME. Calculations from Jeong M1 and Yuan M2 and M3 also attain a relatively high accuracy. When considering only the palm biodiesel with C16:0 below 60 wt% (namely, PME and POME, n = 4), eight of ten models maintain excellent predicting power in terms of AAD and RMSD ≤2. The top three calculation models to reach the highest accuracies were Yuan M1, Chen, and Serrano M1.

This study further examined the robustness of the other CFPP models from categories 3 and 4 and Dunn's proposed model (Dunn, 2020). The prediction results revealed over- or underestimated trends with relatively high numbers of AAD and RMSD (data not shown). However, it is worth to note that Moser M3 and Dunn M2 have the nearest estimated CFPP of PSME (14.3–15.3°C), as listed in Table 2. Moser (2008) utilized the iodine value as a predictor variable which is often used to determine the amount of unsaturation. Dunn (2020) proposed a natural log and reciprocal expression of C16:0 to calculate CFPP. Therefore, the combination of non-linear expression and even iodine value with current prediction models may be suitable approaches to improve their robustness for the challenge of the high content of C16:0 above 60 wt%.

3.3 Cold filter plugging point of palm biodiesel–petrodiesel admixtures

The effect of blending ratio on CFPP for the palm biodiesel with CPC and FPCC petrodiesel fuels is illustrated in Table 3 and Figure 1. The CFPP of palm biodiesel–petrodiesel admixtures increased with higher blend ratio because the saturated FAME content was increased. As shown in Figure 1, the relationship between the blending ratio and CFPP of all palm biodiesel–CPC petrodiesel admixtures was presumably linear or logarithmic at the blending ratio of above 40 vol%. The CFPP of PME and PSME in B40-CPC diesel fuel was 4 and 10 °C and increased to 12 and 16 °C at B70, respectively. The CFPP of POME in B40-CPC is 1 °C, which is significantly lower than that of PME and PSME. Similar trends were observed in palm biodiesel–FPCC petrodiesel admixtures in the range above B40.

At blending ratios below 40 vol%, the measured CFPP apparently departs from the presumable linear lines, as displayed in Figure 1. More importantly, the reduction in CFPP was consistently observed at low blending ratio of B2–B12 among all palm biodiesel–petrodiesel admixtures, in which the blending range is also within the mandated blend levels in most countries. As CFPP was lower than the original value of the neat diesel and biodiesel samples, the depression effect of CFPP can be recognized. The results showed that the CFPPs of B10–B12 for CPC and B2–B12 for FPCC from all six palm biodiesels were consistently lower than the initial CFPP of D100 where CFPPs of CPC and FPCC were −4 and −6, respectively. The most significant depression effect of CFPP was found in B10, in which the CFPP of B10 was −7 to −8°C in CPC and −10 to −13°C in FPCC. Therefore, blending of all six palm biodiesels in B10 substantially reduced about 3–7°C as compared with those of D100 in both petrodiesels.

Undistilled palm biodiesels of PME and POME exhibited a stronger depression effect than their distilled palm biodiesels at the same level of biodiesel–petrodiesel blends. For the blending sample with CPC, CFPPs of B8 PME and PME-D were −8 and −4, respectively, while CFPPs of B8 POME and POME-D were −8 and −5, respectively. For FPCC admixture, CFPPs of B8 were −12 and −7 for PME and PME-D and −15 and −7 for POME and POME-D. In addition,

TABLE 3 CFPPs of distilled and non-distilled palm biodiesels with two major Taiwan diesels (CPC and FPCC) at various blending ratios.

CFPP (°C)	PME	PME-D	PSME	PSME-D	POME	POME-D
CPC (D100/B0 = −4)						
B2	−7	−4	−8	−3	−5	−3
B6	−6	−4	−9	−11	−10	−4
B8	−8	−4	−9	−9	−8	−5
B10	−8	−7	−8	−8	−8	−8
B12	−8	−5	−7	−13	−10	−5
B15	−9	−5	−1	−11	−11	−6
B20	1	−4	−1	1	−9	−7
B30	3	1	5	5	−3	−2
B40	4	6	10	9	1	1
B50	7	8	12	12	5	5
B60	8	9	14	13	8	8
B70	12	11	16	12	9	11
B80	12	10	16	13	11	12
B90	15	14	17	16	13	12
B100	17	18	18	18	12	13
FPCC (D100/B0 = −6)						
B2	−12	−7	−11	−12	−11	−7
B6	−12	−9	−12	−14	−12	−9
B8	−12	−7	−11	−12	−15	−7
B10	−13	−10	−11	−13	−11	−10
B20	−8	−9	−3	−3	−11	−7
B50	5	8	10	10	2	6

Note: Depression effect is defined as the obtained CFPP, lower than D100 and marked in gray.

undistilled palm biodiesels of PME and POME covered wider range of blending ratios for the depression effects. B2–B15 in PME-CPC admixture were observed as the depression effect, while a smaller range of B10–B15 in their distilled forms was identified.

Even though the palm biodiesels have high CFPPs of 13–18°C, which exceed the limit of Taiwanese B100 (CNS 15072), the finding indicated that a low blending of B2–B12 of palm biodiesels can result in a lower and better CFPP of biodiesel–petrodiesel admixture that satisfies the diesel standard CNS 1471 (similar to EN 590).

3.4 Implications of the depression effect of the cold filter plugging point

The depression effect on the cold flow properties has been observed in the CP of saturated fatty esters (Costa et al., 2011) and the PP of n-alkanes with different chain-length combinations (Senra et al., 2009; Senra et al., 2015). On the other hand, in binary mixtures of saturated C16:0 and C18:0 methyl esters, a eutectic reaction with C18:0 at ca. 60–90% C16:0 has been observed on the basis of the solid–liquid phase diagram obtained by differential scanning calorimetry (DSC) (Costa et al., 2011). Senra et al. (2009) and Senra et al. (2015) showed that the trend of PP depression for n-alkane mixtures depends on differences in size and solubility between the long-chain n-alkanes and the added short-chain n-alkane because of their polydispersity and co-crystallization. It should be noted that the CP is the temperature at which nuclei form and that PP is the temperature at which the fuel no longer pours. On the other hand, the CFPP is also defined as the temperature at which crystals grow into large, flat, plate-like structures and begin to adhere to one another, to the extent of filter blockage. Hence, lowering of the CFPP among the studied palm biodiesel–petrodiesel admixture could be mainly due to the suppressed crystal growth and agglomeration, as explained by Sharafutdinov *et al.* (2012). Because visible nuclei have generated from the saturated esters in the palm biodiesels before reaching the CFPP of the neat petrodiesels, these nuclei may interact with the growing petrodiesel waxes by co-crystallizing and agglomerating with the paraffin wax nuclei from the petrodiesel. Thus, this could obstruct crystal growth and agglomeration, although nuclei formation or gelation would

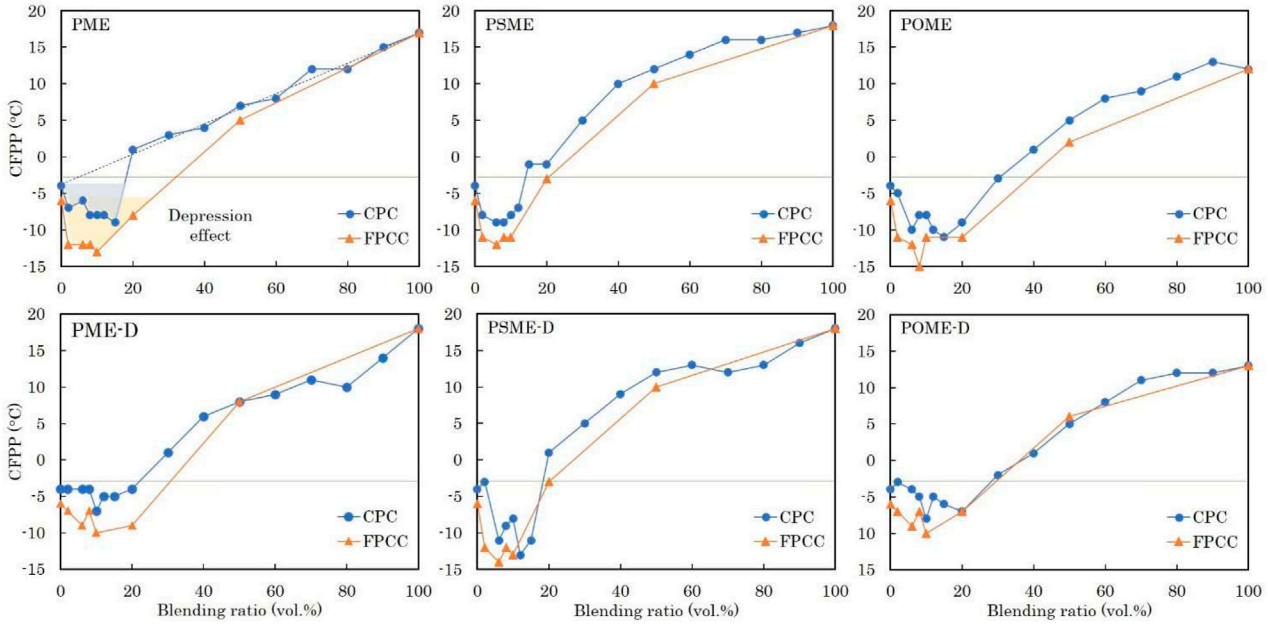

FIGURE 1
CFPP measurements of blending of palm oil methyl esters with two major Taiwan diesels (CPC and FPCC) at various blending ratios. Green lines indicated the CFPP specification (−3°C) of biodiesel–petrodiesel blends in Taiwan CNS 1471.

still occur. Nevertheless, more experimental evidence from co-crystallization process and eutectic reaction in palm biodiesel–petrodiesel admixture system would be theoretically significant to shed light on the depression effect of CFPP.

The results presented here, along with previously published work (Benjumea et al., 2008; Chen et al., 2013; Dunn et al., 1996; Dunn and Bagby, 1995; Kleinová et al., 2007; Moser, 2008; Richards et al., 2007; Sharafutdinov et al., 2012), showed that blending biodiesels with conventional petrodiesel fuels at certain mandated low blend levels does not degrade their cold flow properties in terms of the CFPP. Our findings further suggested that palm biodiesels could be a cold flow improver for Taiwanese petrodiesels at the mandated blending ratio, despite that the palm biodiesels themselves have a CFPP over the limit defined by CNS 15072 (for B100 only). Hence, it might be reasonable to consider two category settings for the CFPP specification of biodiesel, namely, those for direct use as biofuel and for blending components of petrodiesel. In fact, the cold flow property specifications are fairly based on considerable practical purpose or user needs. For instance, in Japanese Biodiesel Standard JIS K 2390:2008, the cold flow properties are not stipulated because the biodiesel specification is used for blending purposes only (JIS K 2204:2007, diesel to B5). In the US, the specifications for the cold flow properties are based on purchase and supply agreements appropriate for the expected ambient temperatures of the region in which the fuel will be used.

4 Conclusion

This study examined the CFPP of six types of palm biodiesels in full blending ratios with two major petrodiesel fuels (CPC and FPCC) in Taiwan. Twelve prediction models of CFPP were evaluated and discussed for their robustness and applicability of neat biodiesel with high palmitic acid content above 60 wt%. The combination of non-linear expression and iodine value with prediction models may be suitable for the CFPP with high content of C16:0 above 60 wt%.

The experimental evidence of CFPP depression effect was obtained for B2–B12 palm biodiesels in both petrodiesel fuels. The most significant depression effect was observed in B10. The CFPP of B10 among all six biodiesels was substantially lower and better than those of D100 in both petrodiesels, in which the CFPP reduction was 3–7°C. At the same level of undistilled and distilled palm biodiesel in CPC petrodiesel, CFPPs of B8 were −8 and −4°C for PME and PME-D and −8 and −5°C for POME and POME-D, respectively. Similar trends were also showed in palm biodiesel-FPCC admixture. Therefore, undistilled palm biodiesels of PME and POME may possess more significant depression effects in terms of wider range of blending ratios and stronger reduction of CFPP.

Although more experimental evidence of co-crystallization process or eutectic reaction could be helpful for a better understanding of the depression effect of CFPP, the current findings revealed that palm biodiesel as a blending component

with conventional petrodiesel fuels at certain mandated low blend levels does not degrade their cold flow properties in terms of the CFPP and is fully justified to meet the diesel standard, for example, CNS 1471. No biofuel feedstocks that are economically and environmentally competitive with palm oils are yet available. The use of blending-purpose palm biodiesel under new regulatory approaches in Taiwan could bring potentially economic, ecological, and environmental benefits.

Data availability statement

The raw data supporting the conclusions of this article will be made available by the authors, without undue reservation.

Author contributions

M-HY: conceptualization, methodology, validation, analysis, writing—original draft, writing—review and editing, funding acquisition, and supervision; Y-HC: conceptualization, methodology, validation, writing—original draft, writing—review and editing, funding acquisition, and supervision; S-CP: conceptualization, methodology, and analysis; L-YC: conceptualization, methodology, and validation; C-YC: conceptualization, methodology, and validation; MS: conceptualization, methodology, validation, and funding acquisition; CA: conceptualization, methodology, validation, and funding acquisition; and Y-FL: validation and resources.

Funding

This work was financially supported by the Ministry of Science and Technology in Taipei, Taiwan (MOST 104-2221-E-027-002-MY3; MOST 105-2221-E-039-011) and the National Taipei University of Technology in Taipei, Taiwan (NTUT-TU-106-01; NTUT-TU-107-01). This study received funding from Chant Oil Co., Ltd., New Taipei City, Taiwan (NTUT 204A061). The funder was not involved in the study design, collection, analysis, interpretation of data, the writing of this manuscript, or the decision to submit it for publication.

Conflict of interest

Y-FL was employed by Chant Oil Co., Ltd.

The remaining authors declare that the research was conducted in the absence of any commercial or financial relationships that could be construed as a potential conflict of interest.

Publisher's note

All claims expressed in this article are solely those of the authors and do not necessarily represent those of their affiliated organizations, or those of the publisher, the editors, and the reviewers. Any product that may be evaluated in this article, or claim that may be made by its manufacturer, is not guaranteed or endorsed by the publisher.

References

Agarwal, A. K. (2007). Biofuels (alcohols and biodiesel) applications as fuels for internal combustion engines. *Prog. Energy Combust. Sci.* 33, 233–271. doi:10.1016/j.pecs.2006.08.003

Benjumea, P., Agudelo, J., and Agudelo, A. (2008). Basic properties of palm oil biodiesel-diesel blends. *Fuel* 87, 2069–2075. doi:10.1016/j.fuel.2007.11.004

Chen, X., Hu, J. M., Chen, L., Li, S., Li, L., Cai, L. L., et al. (2013). Study on cold flow properties of typical materials biodiesel and its blends. *Amr* 781-784, 2383–2388. doi:10.4028/www.scientific.net/amr.781-784.2383

Chen, Y.-H., Chen, J.-H., Chang, C.-Y., and Chang, C.-C. (2010). Biodiesel production from tung (Vernicia Montana) oil and its blending properties in different fatty acid compositions. *Bioresour. Technol.* 101, 9521–9526. doi:10.1016/j.biortech.2010.06.117

Chung, C.-c. (2018). Technological innovation systems in multi-level governance frameworks: The case of Taiwan's biodiesel innovation system (1997-2016). *J. Clean. Prod.* 184, 130–142. doi:10.1016/j.jclepro.2018.02.185

Costa, M. C., Boros, L. A. D., Coutinho, J. A. P., Krähenbühl, M. A., and Meirelles, A. J. A. (2011). Low-temperature behavior of biodiesel: Solid-liquid phase diagrams of binary mixtures composed of fatty acid methyl esters. *Energy fuels.* 25, 3244–3250. doi:10.1021/ef2004199

Demirbas, A. (2009). Political, economic and environmental impacts of biofuels: A review. *Appl. Energy* 86, S108–S117. doi:10.1016/j.apenergy.2009.04.036

Dunn, R. O., and Bagby, M. O. (1995). Low-temperature properties of triglyceride-based diesel fuels: Transesterified methyl esters and petroleum middle distillate/ester blends. *J. Am. Oil Chem. Soc.* 72, 895–904. doi:10.1007/bf02542067

Dunn, R. O. (2020). Correlating the cold filter plugging point to concentration and melting properties of fatty acid methyl ester (biodiesel) admixtures. *Energy fuels.* 34, 501–515. doi:10.1021/acs.energyfuels.9b03311

Dunn, R. O., Shockley, M. W., and Bagby, M. O. (1996). Improving the low-temperature properties of alternative diesel fuels: Vegetable oil-derived methyl esters. *J. Am. Oil Chem. Soc.* 73, 1719–1728. doi:10.1007/bf02517978

Echim, C., Maes, J., and Greyt, W. D. (2012). Improvement of cold filter plugging point of biodiesel from alternative feedstocks. *Fuel* 93, 642–648. doi:10.1016/j.fuel.2011.11.036

Elbehri, A., Segerstedt, A., and Liu, P. (2013). *Biofuels and the sustainability challenge: A global assessment of sustainability issues, trends and policies for biofuels and related feedstocks*. Rome: UN Food and Agriculture Organization.

Gilbert, N. (2012). Palm-oil boom raises conservation concerns. *Nature* 487, 14–15. doi:10.1038/487014a

González Gómez, M. E., Howard-Hildige, R., Leahy, J. J., and Rice, B. (2002). Winterisation of waste cooking oil methyl ester to improve cold temperature fuel properties. *Fuel* 81, 33–39. doi:10.1016/s0016-2361(01)00117-x

Hazrat, M. A., Rasul, M. G., Mofijur, M., Khan, M. M. K., Djavanroodi, F., Azad, A. K., et al. (2020). A mini review on the cold flow properties of biodiesel and its blends. *Front. Energy Res.* 8, 598651. doi:10.3389/fenrg.2020.598651

Hoekman, S. K., Broch, A., Robbins, C., Ceniceros, E., and Natarajan, M. (2012). Review of biodiesel composition, properties, and specifications. *Renew. Sustain. Energy Rev.* 16, 143–169. doi:10.1016/j.rser.2011.07.143

Jambulingam, R., Shankar, V., Palani, S., and Srinivasan, G. R. (2019). Effect of dominant fatty acid esters on emission characteristics of waste animal fat biodiesel in CI engine. *Front. Energy Res.* 7. doi:10.3389/fenrg.2019.00063

Jeong, G.-T., Park, J.-H., Park, S.-H., and Park, D.-H. (2008). Estimating and improving cold filter plugging points by blending biodiesels with different fatty acid contents. *Biotechnol. Bioproc E* 13, 505–510. doi:10.1007/s12257-008-0144-y

Kleinová, A., Paligová, J., Vrbová, M., Mikulec, J., and Cvengros, J. (2007). Cold flow properties of fatty esters. *Process. Saf. Environ.* 85, 390–395.

Knothe, G. (2008). "Designer" biodiesel: Optimizing fatty ester composition to improve fuel properties. *Energy fuels.* 22, 1358–1364. doi:10.1021/ef700639e

Knothe, G. (2009). Improving biodiesel fuel properties by modifying fatty ester composition. *Energy Environ. Sci.* 2, 759–766. doi:10.1039/b903941d

Kongsager, R., and Reenberg, A. (2012). *Contemporary land-use transitions: The global oil palm expansion*. Copenhagen: GLP Report No.4GLP-IPO.

Kung, C.-C., Lan, X., Yang, Y., Kung, S.-S., and Chang, M.-S. (2022). Effects of green bonds on Taiwan's bioenergy development. *Energy* 238, 121567. doi:10.1016/j.energy.2021.121567

Lane, J. (2015). *Biofuels mandates around the world*. Available at: http://www.biofuelsdigest.com/bdigest/2014/12/31/biofuels-mandates-around-the-world-2015 (Accessed December 25, 2021).

Lee, R. A., and Lavoie, J.-M. (2013). From first- to third-generation biofuels: Challenges of producing a commodity from a biomass of increasing complexity. *Anim. Front.* 3, 6–11. doi:10.2527/af.2013-0010

Lim, T. K. (2012). *Edible medicinal and non-medicinal plants*. Dordrecht: Springer. Vol. 1 Fruit.

Lin, C.-Y., and Lu, C. (2021). Development perspectives of promising lignocellulose feedstocks for production of advanced generation biofuels: A review. *Renew. Sustain. Energy Rev.* 136, 110445. doi:10.1016/j.rser.2020.110445

Liu, G. (2015). Development of low-temperature properties on biodiesel fuel: A review. *Int. J. Energy Res.* 39, 1295–1310. doi:10.1002/er.3334

Luque, R., Lovett, J. C., Datta, B., Clancy, J., Campelo, J. M., and Romero, A. A. (2010). Biodiesel as feasible petrol fuel replacement: A multidisciplinary overview. *Energy Environ. Sci.* 3, 1706–1721. doi:10.1039/c0ee00085j

Moser, B. R. (2008). Influence of blending canola, palm, soybean, and sunflower oil methyl esters on fuel properties of biodiesel. *Energy fuels.* 22, 4301–4306. doi:10.1021/ef800588x

Najjar, Y. S. H., and Abu-Shamleh, A. (2020). Harvesting of microalgae by centrifugation for biodiesel production: A review. *Algal Res.* 51, 102046. doi:10.1016/j.algal.2020.102046

OECD/FAO (2021). *OECD-FAO agricultural outlook 2021-2030*. Paris: OECD Publishing. doi:10.1787/19428846-en

Pan, H., Liu, Y., Xia, Q., Zhang, H., Guo, L., Li, H., et al. (2020). Synergetic combination of a mesoporous polymeric acid and a base enables highly efficient heterogeneous catalytic one-pot conversion of crude Jatropha oil into biodiesel. *Green Chem.* 22, 1698–1709. doi:10.1039/c9gc04135d

Pan, H., Xia, Q., Li, H., Wang, Y., Shen, Z., Wang, Y., et al. (2022). Direct production of biodiesel from crude Euphorbia lathyris L. Oil catalyzed by multifunctional mesoporous composite materials. *Fuel* 309, 122172. doi:10.1016/j.fuel.2021.122172

Richards, P., Reid, J., Tok, L. H., and MacMillan, I. (2007). The emerging market for biodiesel and the role of fuel additives. *SAE Technical Paper 2007-01-2033*. Warrendale, PA: SAE International. doi:10.4271/2007-01-2033

Sarin, A., Arora, R., Singh, N. P., Sarin, R., Malhotra, R. K., and Sarin, S. (2010). Blends of biodiesels synthesized from non-edible and edible oils: Effects on the cold filter plugging point. *Energy Fuel* 24, 1996–2001. doi:10.1021/ef901131m

Senra, M., Grewal, M. G., and Jarboe, J. H. (2015). The role of n-alkane solvent carbon number on the gelation of long-chained n-alkanes in solution. *Ind. Eng. Chem. Res.* 54, 4505–4511. doi:10.1021/ie504083y

Senra, M., Scholand, T., Maxey, C., and Fogler, H. S. (2009). Role of polydispersity and cocrystallization on the gelation of long-chainedn-alkanes in solution. *Energy fuels.* 23, 5947–5957. doi:10.1021/ef900652e

Serrano, M., Oliveros, R., Sanchez, M., Moraschini, A., Martínez, M., and Aracil, J. (2014). Influence of blending vegetable oil methyl esters on biodiesel fuel properties: Oxidative stability and cold flow properties. *Energy* 65, 109–115.

Sharafutdinov, I., Stratiev, D., Shishkova, I., Dinkov, R., Batchvarov, A., Petkov, P., et al. (2012). Cold flow properties and oxidation stability of blends of near zero sulfur diesel from Ural crude oil and FAME from different origin. *Fuel* 96, 556–567. doi:10.1016/j.fuel.2011.12.062

Yuan, M.-H., Chen, Y.-H., Chen, J.-H., and Luo, Y.-M. (2017). Dependence of cold filter plugging point on saturated fatty acid profile of biodiesel blends derived from different feedstocks. *Fuel* 195, 59–68. doi:10.1016/j.fuel.2017.01.054